MECHANICAL MODEL OF BIOLOGICAL SUTURES WITH FIBROUS JOINTS

Kateryna Miroshnichenko[1], Lei Liu[2], Igor Tsukrov[3*], and Yaning Li[4*]

[1,2,3,4] 33 College Road, Mechanical Engineering Department,
University of New Hampshire, Durham NH, USA
[3] Igor.Tsukrov@unh.edu
[4] Yaning.Li@unh.edu

Keywords: Cranial sutures, Fiber reinforced composites,
Anisotropic mechanical properties, Biological joints
*corresponding authors

ABSTRACT

Biological sutures are mechanical joints connecting skeletal components with a thin interfacial layer of soft connective tissue, showing a complicated zigzag morphology. The interfacial layer is composed of aligned collagen fibers embedded in mesenchyme matrix. Biological sutures have multiple mechanical functions to provide protection by effectively transmitting load and dissipating energy, while also to supply flexibility by accommodating growth, respiration and locomotion.

Recently, theoretical models were developed to predict the stiffness and strength of sutures with various wavy morphologies. In these theoretical models, the soft interfacial layer was assumed to be isotropic. However, due to the aligned collagen fibers in the interfacial layer, the effective mechanical properties of the layer are anisotropic. Therefore, it is not clear how the anisotropic properties of the fibrous interfacial layer and the wavy suture morphology jointly influence the mechanical properties of biological sutures.

In this investigation, a composite suture model is developed in order to provide better understanding of the synergistic effects of suture morphology and the fiber orientation in the soft connective tissue. The model includes a soft thin interfacial layer connecting two bone pieces with saw tooth geometry. The layer is modeled as aligned fibers embedded in soft matrix. Therefore, the interfacial layer in the model is anisotropic, and its properties are determined by the fiber orientation, fiber volume fraction, and the mechanical properties of the fibers and the matrix. This theoretical mechanical model was used to systematically quantify the overall orthotropic in-plane stiffness of suture joints as a function of wavy morphology of the skeletal components, the fiber orientation, and matrix properties in the interfacial layer.

1 INTRODUCTION

Biological sutures are important composite joints connecting skeletal components with a thin layer of soft tissue. They are found in many biological systems, such as the cranial sutures of vertebrate skulls [1-3], the pelvic suture of the armored fish *Gasterosteus aculeatus* (the three-spined stickleback) [4], the sutures on the carapace of the red-eared slider turtle [5]. Biological sutures have multiple mechanical functions to provide protection by effectively transmitting load and dissipating energy, and also provide flexibility to accommodate growth, respiration and locomotion [1-2, 6-11]. For example, Finite Element (FE) simulations have shown that the introduction of suture joints into a FE model of the cranium can change the magnitude and the patterns of strain across the cranium [12-15].

The unique mechanical properties and multi-function of sutures are due to the synergistic effects of the complex zigzag geometry of the skeleton and the interfacial layer, and the fibrous structure of the connective tissue. On the one hand, most of the biological sutures have interdigitated wavy morphology to facilitate load transmission and energy dissipation [1-2, 9, 11, 16-18]. On the other hand, in the connective interfacial layer, aligned collagen fibers are found embedded in soft

mesenchyme matrix to provide connection and flexibility between skeletal parts and absorbing energy [3, 19].

Recently, to explore the influence of wavy morphology on the overall mechanical properties of biological sutures, sophisticated theoretical models were developed to predict the stiffness and strength of sutures with single-waved and hierarchical triangular saw tooth geometry [16, 20]. It was proven that the triangular tooth geometry optimizes advantages in load transmission, weight, stiffness, strength, energy absorption and fatigue. The model predictions were further verified via FE simulations on sutures with general trapezoidal teeth [17] and mechanical experiments on 3D printed specimens [21]. These theoretical models provided fundamental understanding on how suture morphology influences the overall mechanical properties of sutures. However, the fibrous microstructure of the soft interfacial layer was not considered and the layer was assumed to be isotropic. To study the influences of aligned collagen fibers on the stiffness of biological sutures, 2D FE models with anisotropic layer properties were employed [19]. The modeling results demonstrated that the arrangement of collagen fibers and suture morphology jointly optimize the suture response under compressive and tensile loads.

This paper presents a theoretical mechanical model developed to systematically explore the synergistic effects of suture morphology and the fibrous structure of soft connective tissue. In the model, the overall in-plane stiffness of suture joints is determined by the wavy morphology of sutures, the fiber orientation, fiber volume fraction, and the mechanical properties of fibers and matrix in the interfacial layer. The rest of the paper is organized in four major sections including problem formulation, theoretical modeling, results, and conclusions.

2 PROBLEM FORMULATION

The geometry of the composite suture model is shown in Fig. 1a. The light blue color represents the skeletal parts and the zigzag yellow layer represents the soft connective tissue. The skeletal teeth are considered as triangular with tooth tip angle of 2θ. When the thickness of the interfacial layer changes, the volume fraction of skeleton f will vary accordingly. In the model, three coordinate systems are defined: the first one is the global coordinate system X-Y, in which Y is normal to the general direction of the suture; the second one is the local coordinate system n-t, in which n is along the normal direction of the interfacial layer, and t is tangential to the interfacial layer, the third one is the fiber coordinate system x-y, it is assumed that the fibers are parallel to each other and aligned in the direction x. The orientation of collagen fibers is defined by angle β, which is the clockwise angle between the unit vector $\boldsymbol{n}$ and the fiber direction x as shown in Figs. 1a and 1b in 2D and 3D views, respectively. In the model, β can change from 0^o (when fibers are perpendicular to the interface) to 180^o. The suture model is subjected to far-field stress that corresponds to surface traction $\bar{\boldsymbol{\sigma}}$ at the boundaries. The surface traction is described as $\bar{\boldsymbol{\sigma}} = (\sigma_X, \sigma_Y, \sigma_{XY})$ in the global coordinate system.

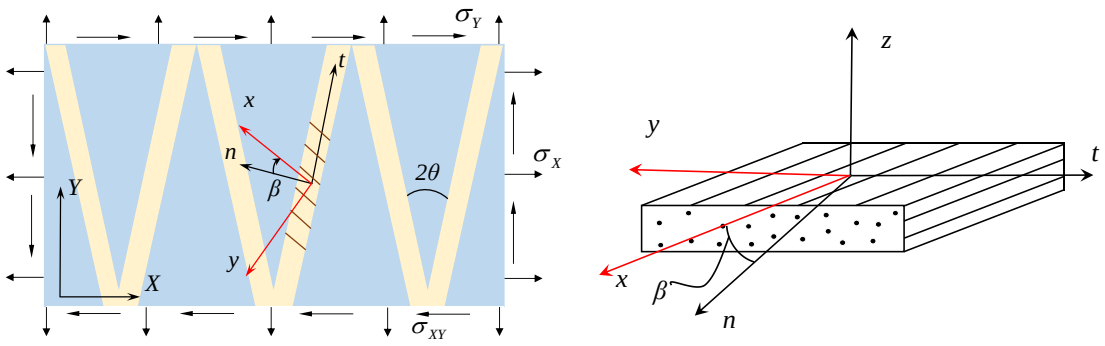

(a) (b)

Fig. 1: (a) Schematic graph of the composite suture model, and (b) the 3D view of the interfacial layer.

3 THEORETICAL MODELING

3.1 Overall stiffness of sutures

The mechanical properties of each component are defined as: the Young's modulus E_b and the shear modulus G_b of the skeletal phase; the Young's modulus E_m and Poisson's ratio v_m of the soft mesenchyme matrix; the Young's modulus E_f and the Poisson's ratio v_f of the collagen fibers. For biological sutures, these properties can be found in literature as: E_b = 6 GPa and the Poisson's ratio v_b = 0.27 [19]; E_m = 12 MPa and v_m = 0.45; E_f = 360 MPa [22] and v_f = 0.3 [23]. The volume fraction of skeleton was taken as f = 85%. Because the fibers in the interfacial layer are assumed to be aligned, the interfacial layer is transversely isotropic. In the fiber coordinate system x-y, the effective moduli of the interfacial layer (E_x, E_y, and G_{xy}) and the Poisson's ratios (v_{xy}, v_{yx}) are determined by the fiber orientation β, fiber volume fraction f_f, and the mechanical properties of the fibers and the matrix (E_m, E_f, v_m, v_f). In literature, f_f varies between 0.15-0.42. In this study, we selected the average value of f_f =0.285. In the local coordinate system n-t, the effective moduli of the interfacial layer (E_n, E_t, and G_{nt}) and the Poisson's ratios (v_{nt}, v_{tn}) are determined from (E_x, E_y, G_{xy}, v_{xy}, v_{yx}), and β by coordinate transformation.

Therefore, the composite suture is orthotropic and the effective moduli (E_X, E_Y and G_{XY}) can be derived as functions of tooth tip angle θ, the stiffness of skeleton E_b, volume fraction of skeleton f, and the effective moduli of the interfacial layer (E_n, E_t, and G_{nt}) as:

$$E_X = \left[(1-f)\left(\frac{\cos^2\theta \sin^2\theta}{G_{nt}} + \frac{\cos^4\theta}{E_n} + \frac{\eta_{sn}\sin\theta\cos^3\theta}{G_{nt}} + \frac{\eta_{ns}\sin\theta\cos^3\theta}{E_n} \right) + \frac{f}{E_b} \right]^{-1}, \quad (1)$$

$$E_Y = \frac{f^2 E_b}{(1-f)\left(\frac{E_b}{G_{nt}}\sin^2\theta\cos^2\theta + \frac{E_b}{E_n}\sin^4\theta + E_b\left(\frac{\eta_{sn}\cos\theta\sin^3\theta}{G_{nt}} + \frac{\eta_{ns}\cos\theta\sin^3\theta}{E_n} \right) \right) + f}, \quad (2)$$

where E_n is the effective normal stiffness of the interface layer. Due to anisotropy of the interfacial layer, its shearing and tensile deformation are always coupled and η_{ns}, η_{sn} in equations (1) and (2) are the coupling coefficients expressed as [24]:

$$\eta_{sn} = G_{nt}\left(\frac{2mn^3}{E_x}(1+\nu_{xy}) - \frac{2m^3 n}{E_y}(1+\nu_{yx}) + \frac{mn(m^2-n^2)}{G_{xy}} \right), \quad (3)$$

$$\eta_{ns} = \eta_{sn}\frac{E_n}{G_{nt}}, \quad (4)$$

where, $m = \sin\beta$, $n = \cos\beta$, and ($E_x, E_y, G_{xy}, \nu_{yx}, \nu_{xy}$) are the transversely isotropic properties of the interfacial layer.

The overall shear modulus of suture can be written as [17, 21]:

$$G_{XY} = \frac{f^2 c E_n E_b}{f c c^b E_n + (1-f)(1+c^\gamma)E_b}, \quad (5)$$

where c, c^b, c^γ are non-dimensional parameters expressed as:

$$c = \frac{G_{nt}}{E_n} + \frac{E_n^{ps}}{E_n}\left(\tan\theta\right)^{-2}, \tag{5a}$$

$$c^b = \frac{3E_b}{4G_b} + \frac{5}{16}\left(\tan\theta\right)^{-2}, \tag{5b}$$

$$c^\gamma = \frac{3G_{nt}}{2G_b} + \frac{9G_{nt}}{8E_b}\left(\tan\theta\right)^{-2}, \tag{5c}$$

3.2 Effective stiffness of the fibrous interfacial layer

The effective stiffness of the interfacial layer in the local coordinate system *n-t* is related to that in the fiber coordinate system *x-y* as:

$$\frac{1}{E_t} = \frac{m^2}{E_x}\left(m^2 - n^2\nu_{xy}\right) + \frac{n^2}{E_y}\left(n^2 - m^2\nu_{yx}\right) + \frac{m^2n^2}{G_{xy}}, \tag{6}$$

$$\frac{1}{E_n} = \frac{n^2}{E_x}\left(n^2 - m^2\nu_{xy}\right) + \frac{m^2}{E_y}\left(m^2 - n^2\nu_{yx}\right) + \frac{m^2n^2}{G_{xy}}, \tag{7}$$

$$\frac{1}{G_{nt}} = \frac{4m^2n^2}{E_x}\left(1+\nu_{xy}\right) + \frac{4m^2n^2}{E_y}\left(1+\nu_{yx}\right) + \frac{\left(m^2-n^2\right)^2}{G_{xy}}, \tag{8}$$

where the transversely isotropic properties of the interfacial layer ($E_x, E_y, G_{xy}, \nu_{yx}, \nu_{xy}$) in the fiber coordinate *x-y* can be obtained through Voigt law, Reuss law, and Maxwell's reciprocal theorem as:

$$E_x = f_f E_f + \left(1 - f_f\right)E_m, \tag{9}$$

$$E_y = \left(\frac{f_f}{E_f} + \frac{1-f_f}{E_m^{ps}}\right)^{-1}, \tag{10}$$

$$G_{xy} = \left(\frac{f_f}{G_f} + \frac{1-f_f}{G_m}\right)^{-1}, \tag{11}$$

$$\nu_{xy} = \nu_f f_f + \left(1 - f_f\right)\nu_m, \tag{12}$$

$$\nu_{yx} = \frac{E_y}{E_x}\nu_{xy}, \tag{13}$$

where $E_m^{ps} = \dfrac{E_m}{1-\nu_m^2}$ is the plane-strain stiffness of the matrix, and f_f is the volume fraction of fibers in the interfacial layer. Thus, through Eqs. (1–13), with the mechanical properties chosen from literature for each material component, the effective moduli (E_X, E_Y and G_{XY}) can be numerically determined as functions of θ and β.

4 RESULTS

The overall moduli (E_X, E_Y and G_{XY}) of suture joints predicted from Eqs. (1), (2) and (5) are plotted in Fig. 2 as functions of fiber orientation β for four tooth tip angles, θ =10°, 30°, 45°, and 60°. It can be seen that longitudinal stiffness E_Y, in almost the entire range of β (except for β <~30°) increases when θ decreases. There are two peaks on $E_Y - \beta$ curve, the first peak is when β is between 0° – 90° (specifically, at β =42.5°, 39.5°, 38.4°, and 33.2°, for θ =10°, 30°, 45°, and 60°, respectively) and the second is when β is between 90° – 180° (specifically, at β =133°, 129.5°, 128.3°, and 123.8°, for θ =10°, 30°, 45°, and 60°, respectively). E_Y reaches the lowest value when the fibers are either perpendicular to the interface (β = 0° or 180°) or parallel to the interface (β = 90°). The three valley are almost the same: E_Y = 958, 953 and 951 MPa at β = 0°, 90°, and 176.5°, respectively. Also, the two peaks are different in magnitude. For example, for θ =10°, the two peaks are E_Y = 1915 MPa and 1714 MPa at β = 43°, 133.5° respectively. The second peak is lower than the first one due to the anisotropy-induced coupling between shear and tensile deformation in the interfacial layer, as shown in Eqs. (1-4).

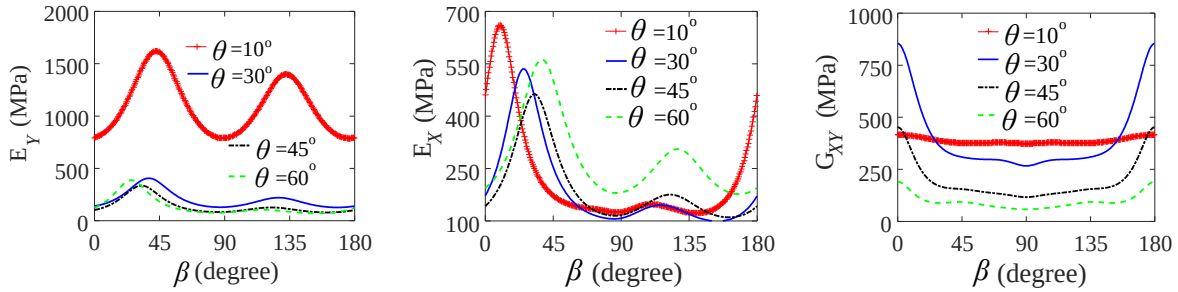

Fig. 2: Effective moduli of sutures with different tooth tip angel θ, and different fiber orientation β.

E_X changes in a very large range with β. For θ =30°, 45°, and 60°, there are two peaks on the $E_X - \beta$ curves, but not for θ =10°. The highest value of E_X is obtained when β is between 0° – 45° (specifically, at β =10.3°, 22.9°, 26.4°, and 33.2°, when θ = 10°, 30°, 45°, and 60°, respectively). The second peak is much smaller than the first one.

G_{XY} reaches the highest values at β =0° and 180°, i.e. when the fibers are perpendicular to the interface, and reaches the lowest values at β = 90° when the fibers are parallel to the interface. For θ = 10°, G_{XY} only slightly varies with β. For larger θs, when β is smaller than 45°, G_{XY} decreases dramatically when β increases; when β is larger than 135°, when β increases, G_{XY} increases dramatically; when β is between 45° and 135°, G_{XY} only slightly varies with β.

The dependence of (E_X, E_Y and G_{XY}) on the fiber orientation β is attributed to the β-induced anisotropic effective properties of the interfacial layer. According to Eqs. (6) – (8), the effective moduli (E_n, E_t, and G_{nt}) of the interfacial layer are plotted as functions of β in Fig. 3a. It can be seen that E_n reaches its maximum when β = 0° and 180° while E_t reaches its maximum when β = 90°. G_{nt} reaches the peaks at 45° and 135°, and has minimum values at β = 0°, 90°, and 180°. Generally, E_t has little influence on (E_X, E_Y, or G_{XY}). As shown in Eqs. (1-2), when θ < 45°, G_{nt} has larger influence on E_Y than E_n, and E_n has a larger influence on E_X than G_{nt}; when θ > 45°, E_n has a larger influence on E_Y than G_{nt}, and G_{nt} has a larger influence on E_X than E_n.

The anisotropy-induced coupling coefficients, η_{sn} and η_{ns} are plotted as functions of β in Fig.3b. The coupling coefficients quantify interaction between the shearing and normal deformation. The shearing stress can generate normal deformation, and the normal stress also generates shearing deformation. It can be seen that they are zeros at β =0°, 57°, 90°, 123° and 180°. Therefore, no coupling effects are present at these five fiber orientations. When β is between 0° and 57°, and 90° and 123°, η_{ns} is negative; when β is between 57° and 90°, and 123° and 180°, η_{ns} is positive. Similar behavior is observed for η_{sn} with a smaller amplitude, as shown in Fig.3b.

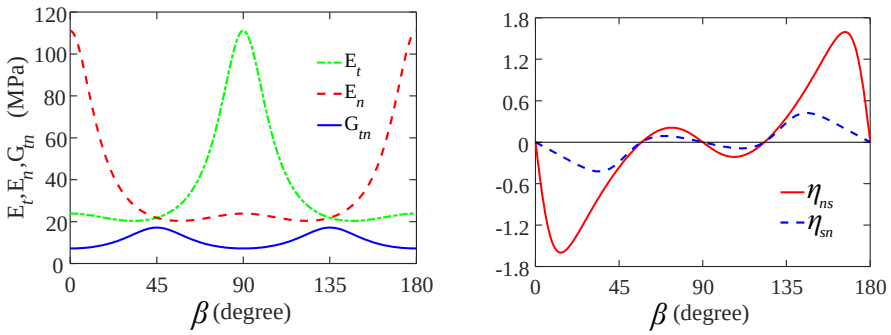

(a) (b)

Fig. 3: (a) The effective elastic moduli of the interfacial layer for various fiber orientation β; and (b) the coupling coefficients of the interfacial layer as functions of β.

The Young's modulus of mesenchyme matrix in the interfacial layer also plays an important role in determining the overall stiffness of sutures. The overall stiffness of sutures with different matrix stiffness (E_m = 120 MPa, 12 MPa and 1.2 MPa) are plotted in Fig.4 as functions of θ. In general, when E_m increases, the overall stiffness increases. For G_{XY}, when θ is small, E_m barely influences G_{xy}; while when θ is large, E_m significantly influences G_{XY}, as shown in Fig.4c. Also, it is further confirmed that when θ is small, E_Y and G_{XY} are sensitive to θ, as shown in Figs.4a and 4c: when θ increases, E_Y dramatically decreases, while G_{XY} increases. There is a critical value of θ which corresponds to the maximum value of G_{XY}, and when E_m increases, this critical value of θ increases, as shown in Fig. 4c. E_x only slightly varies when θ changes, as shown in Fig.4b.

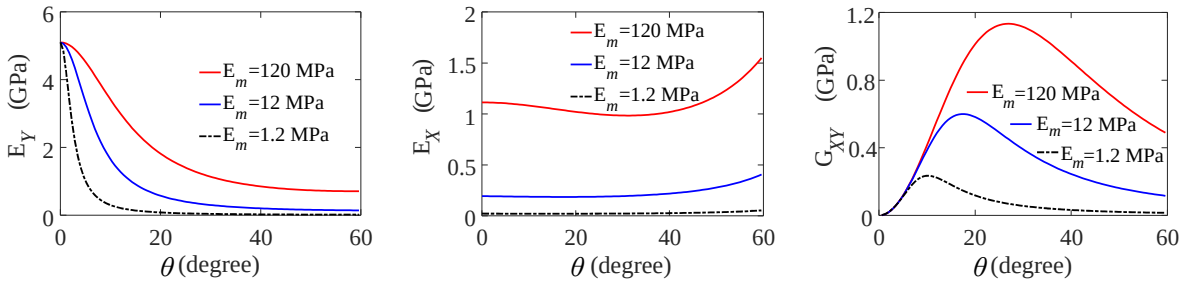

(a) (b) (c)

Fig. 4 Overall moduli of sutures vs. tooth tip angle θ for different values of matrix stiffness E_m, with β =45°: (a) E_Y, (b) E_X, and (c) G_{XY}.

5 CONCLUSIONS

The mechanical properties of biological sutures with aligned collagen fibers in the interfacial layer between two skeleton pieces were predicted via a composite suture model. Theoretical mechanical model was developed to consider the influence of fiber orientation β on the effective properties of sutures. The influence was systematically quantified for various suture morphologies determined by the tooth tip angle θ. The model was also used to study the influence of the stiffness of the mesenchyme matrix in the interfacial layer on the overall suture properties.

It was found that the overall stiffness of suture is determined by the tooth tip angle, and the effective normal and shear moduli (E_n and E_{nt}, respectively) of the interfacial layer. The fiber orientation β significantly influences the effective stiffness of the interfacial layer and therefore the overall stiffness of sutures. Generally, when the tooth tip angle decreases and the stiffness E_m of the soft mesenchyme matrix increases, the effective moduli of sutures increase. Although, when the tooth

tip angle 2θ of the suture is small (less than ~15 degrees), the matrix stiffness barely influences the overall shear modulus G_{XY} of sutures.

In the range of material parameters chosen from literature, the overall longitudinal stiffness E_Y of sutures reaches two peaks around $\beta = 45^o$, and $\beta = 135^o$. The first peak around $\beta = 45^o$ is higher than the second peak around $\beta = 135^o$; and the minimum values of E_Y is obtained at $\beta = 0^o$, 90^o, and 180^o, i.e. when the fibers are either perpendicular or parallel to the interface between the skeleton and the connective layer. For sutures with sharp teeth ($\theta < 10^o$), the two peaks of E_Y are obtained when β is very close to 45^o and 135^o. When the tooth tip angle θ increases beyond 10^o, the critical fiber orientation β corresponding to the peaks of E_Y becomes smaller and smaller than 45^o, and 135^o.

When $\theta < 45^o$, G_{nt} has more influence on E_Y than E_n, and E_n has more influence on E_X than G_{nt}; when $\theta > 45^o$, E_n has more influence on E_Y than G_{nt} , and G_{nt} has more influence on E_X than E_n. For G_{XY}, when θ is small ($\theta < 10^o$), it is barely influenced by the fiber orientation β; when θ is above 10^o, G_{XY} - β curve is symmetric about $\beta = 90^o$. G_{XY} reaches maximum when the fibers are perpendicular to the interface, and then dramatically decreases and reaches its lowest value at $\beta = 90^o$, i.e. when fibers are parallel to the interface.

ACKNOWLEGEMENTS

This work was supported by National Science Foundation (NSF) under grant 1362893, and US Air Force Office of Scientific Research (AFOSR) under grant FA9550-16-1-0011, and the CEPS fellowship at University of New Hampshire (UNH).

REFERENCES

[1] R.P. Hubbard, J.W. Melvin, I.T. Barodawa, Flexure of Cranial Sutures, *Journal of Biomechanics*, **4**, 1971, pp. 491-496.

[2] C.R. Jaslow, Mechanical Properties of Cranial Sutures, *Journal of Biomechanics*, **23 (4)**, 1990, pp. 313-321.

[3] K.L. Rafferty, S.W. Herring, Craniofacial sutures: morphology, growth, and in vivo masticatory strains, *Journal of Morphology*, **242 (2)**, 1999, pp. 167-179.

[4] J.H. Song, S. Reichert, I. Kallai, D. Gazit, M. Wund, M.C. Boyce, C. Ortiz, Quantitative microstructural studies of the armor of the marine threespine stickleback (Gasterosteus aculeatus), *Journal of Structural Biology*, **171 (3)**, 2010, pp. 318-331.

[5] S. Krauss, E. Monsonego-Ornan, E. Zelzer, P. Fratzl, R. Shahar, Mechanical Function of a Complex Three-Dimensional Suture Joining the Bony Elements in the Shell of the Red-Eared Slider Turtle, *Advanced Materials*, **21 (4)**, 2009, pp. 407- 412.

[6] E. Mclaughlin, Y. Zhang, D. Pashley, J. Borke, J. Yu, The load-displacement characteristics of neonatal rat cranial sutures, *The Cleft Palate-Craniofacial Journal*, **37 (6)**, 2000, pp. 590-595.

[7] S.S. Margulies, K.L. Thibault, Infant skull and suture properties: measurements and implications for mechanisms of pediatric brain injury, *Journal of Biomechanical Engineering*, **122 (4)**, 2000, pp. 364-371.

[8] B. Coats, S.S. Margulies, Material properties of human infant skull and suture at high rates, *Journal of Neurotrauma*, **23 (8)**, 2006, pp. 1222-12321.

[9] T.E. Popowics, S.W. Herring, Load transmission in the nasofrontal suture of the pig, Sus scrofa, *Journal of Biomechanics*, **40 (4)**, 2007, pp. 837-844.

[10] M. T. Davis, A. M. Loyd, H. yu H. Shen, M. H. Mulroy, R. W. Nightingale, B. S. Myers, C. D. Bass, The mechanical and morphological properties of 6 year-old cranial bone, *Journal of Biomechanics*, **45 (15)**, 2012, pp. 2493–2498.

[11] A. Maloul, J. Fialkov, C.M. Whyne, Characterization of the bending strength of craniofacial sutures, *Journal of Biomechanics*, **46 (5)**, 2013, pp. 912–917.

[12] E.J. Rayfield, Cranial mechanics and feeding in Tyrannosaurus rex, *Proceedings of The Royal Society*, **B 271 (1547)**, 2004, pp. 1451–1459.

[13] E.J. Rayfield, Aspects of comparative cranial mechanics in the theropod dinosaurs Coelophysis, Allosaurus and Tyrannosaurus. Zool, *Botanical Journal of the Linnean Society*, **144**, 2005, pp. 309–316.
[14] K. Kupczik, C.A. Dobson, M. J. Fagan, R. H. Crompton, C. E. Oxnard, P. O'Higgins, Assessing mechanical function of the zygomatic region in macaques: validation and sensitivity testing of finite element models, *Journal of Anatomy*, **210**, 2007, pp. 41–53.
[15] M. Moazen, N. Curtis, P. O'Higgins, M.E.H. Jones, S.E. Evans, M.J. Fagan, Assessment of the role of sutures in a lizard skull: a computer modelling study, *Proceedings of the royal society*, **B 276**, 2009, pp. 39-46.
[16] Y. Li, C. Ortiz, M.C. Boyce, Stiffnes and strength of a suture joint model, *Physical Review*, **E 84 (6)**, 2011, 062904.
[17] Y. Li, C. Ortiz, M.C. Boyce, A generalized mechanical model for suture interfaces of arbitrary geometry, *Journal of Mechanics and Physics of Solids*, **61 (4)**, 2013, 1144-1167.
[18] E. Lin, Y. Li, J.C. Weaver, C. Ortiz, M.C. Boyce, Tunability and enhancement of mechanical behavior with additively manufactured bio-inspired hierarchical suture interfaces, *Journal of Materials Research*, **9 (17)**, 2014, pp. 1867-1875.
[19] S.C. Jasinoski, B.D. Reddy, K.K. Louw, & A. Chinsamy, Mechanics of cranial sutures using the finite element method, *Journal of Biomechanics*, ***43*(16)**, 2010, pp. 3104–3111.
[20] Y. Li, C. Ortiz, M.C. Boyce, Bioinspired, mechanical, deterministic fractal model for hierarchical suture joints, *Physical Review*, **E 85(3)**, 2012, 031901.
[21] E. Lin, Y. Li, C. Ortiz, M.C. Boyce, 3D printed, bio-inspired prototypes and analytical models for structured suture interfaces with geometrically-tuned deformation and failure behavior, *Journal of the Mechanics and Physics of Solids*, **73**, 2014, pp. 166-182.
[22] E. Gentleman, A.N. Lay, D.A. Dickerson, E.A. Nauman, G.A. Livesay, K.C. Dee, Mechanical characterization of collagen fibers and scaffolds for tissue engineering, *Biomaterials*, **24 (21)**, 2003, pp. 3805-13.
[23] S.M. Elhamian, M. Alizadeh, M. Mehrdad Shokrieh, A. Karimi, S.P. Madani, The effect of collagen fibers volume fraction on the mechanical properties of articular cartilage by micromechanics models, *Perfusion*, **30 (7)**, 2014, pp. 1-9.
[24] I.M. Daniel, O. Ishai, *Engineering Mechanics of Composite Materials*, Oxford University Press, 2nd edition, 2006.